J. Synchrotron Rad. (1998). **5**, 874–876

New methods for semiconductor charge-diffusion-length measurements using synchrotron radiation

J. Kohagura,[a]* T. Cho,[a] M. Hirata,[a] T. Okamura,[a] T. Tamano,[a] K. Yatsu,[a] S. Miyoshi,[a] K. Hirano[b] and H. Maezawa[b]

[a]Plasma Research Centre, University of Tsukuba, Ibaraki 305, Japan, and [b]Photon Factory, Institute of Material Structure Science, High Energy Accelerator Research Organization, Ibaraki 305, Japan.
E-mail: kohagura@prc.tsukuba.ac.jp

(*Received 4 August 1997; accepted 21 November 1997*)

The extension of a new theory on the X-ray energy response of semiconductor detectors is carried out to characterize the X-ray response of a multichannel semiconductor detector fabricated on one silicon wafer. Recently, these multichannel detectors have been widely utilized for position-sensitive observations in various research fields, including synchrotron radiation research and fusion-plasma investigations. This article represents the verification of the physics essentials of a proposed theory on the X-ray response of semiconductor detectors. The three-dimensional charge-diffusion effects on the adjoining detector-channel signals are experimentally demonstrated at the Photon Factory for two types of multichannel detectors. These findings are conveniently applicable for measuring diffusion lengths for industrial requirements.

Keywords: X-ray detectors; multichannel detectors; diffusion lengths; semiconductor detectors; X-ray response theory.

1. Introduction

Our newly proposed theory on the energy response of a semiconductor X-ray detector (Cho *et al.*, 1992, and see §2) has solved the serious problem of a recent finding of the invalidity (Wenzel & Petrasso, 1988) of the conventional standard theory (Price, 1964); that is, it is claimed that the X-ray energy response is not interpreted by the conventional and widely utilized theory, employed over the last quarter of the century, using the depletion-layer thickness as an X-ray sensitive layer. In addition, recent underbiased operations of multichannel semiconductor detectors for plasma X-ray tomographic reconstructions enhance the importance of the correct use of the X-ray response theory, since such an operational method is widely employed in various plasma-confinement devices in order to avoid detector breakdown due to fusion-produced neutron damages.

2. The three-dimensional charge-diffusion effect on output signals of a multichannel semiconductor detector

In this section, we discuss the three-dimensional analysis of the diffusion process of X-ray-produced carriers in a silicon field-free substrate using our novel theory on the quantum efficiency of a semiconductor X-ray detector. This method becomes essentially of importance when we estimate the diffusion effect (Hopkinson, 1983) on adjoining channels of a multichannel detector.

The three-dimensional diffusion equation for a charge flux, φ, created in a substrate by X-rays is described as

$$\frac{1}{r^2}\frac{\mathrm{d}r^2}{\mathrm{d}r}\frac{\mathrm{d}\varphi(r)}{\mathrm{d}r} - \frac{1}{L^2}\varphi(r) = -\frac{s(d)}{D}, \tag{1}$$

where the minority carrier diffusion length L is written as $L^2 = D/\Sigma$; Σ is the charge-recombination coefficient and D is the diffusion coefficient of the charge. The source charge, s, is created by incident X-rays at a depth d from the upper surface of the diffusion region, and the distance r is defined as $r^2 = x^2 + y^2 + z^2$ (see Fig. 1*a*). Here, we define a flow density of the charge as $J(r)$ in the following,

$$J = -D(\mathrm{d}\varphi/\mathrm{d}r) = (s/4\pi r^2)(r/L + 1)\exp(-r/L), \tag{2}$$

where

$$s = I_1(E/\varepsilon)\mu\rho = I_0(E/\varepsilon)\mu\rho\exp(-\mu\rho d). \tag{3}$$

Here, I_0 and I_1 are the X-ray intensities with an energy E at the upper surface of the substrate ($z = 0$), and at a depth of d, respectively. ε is the energy required to create an electron–hole pair, and μ and ρ denote the silicon mass-absorption coefficient and the mass density, respectively.

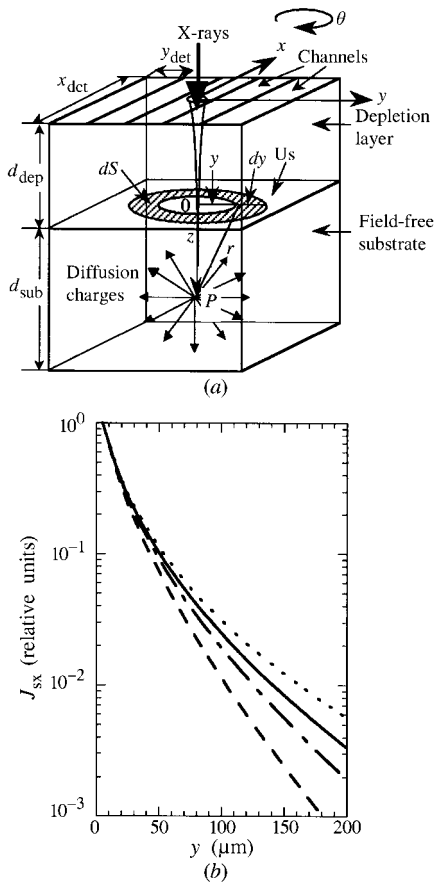

Figure 1
(*a*) A multichannel semiconductor X-ray detector along with the diffusing charges from an X-ray absorption point in the field-free substrate. X-rays are injected at $x = y = 0$. (*b*) The dashed, dot-dashed, solid and dotted curves represent the diffusion signals $J_{sx}(y)$ calculated from our three-dimensional diffusion theory [see equation (6)] for a unit-intensity X-ray at 5 keV using L = 50, 75, 100 and 150 μm, respectively.

For the purpose of a display of the diffusion-charge profile in the y direction, X-rays are injected at $y = 0$ along the z axis (Fig. 1).

The signal contribution due to charge diffusing from P to an area dS in Fig. 1(a), $dQ_{\rm dif}(y)$, is described using $J(r)$ as

$$\mathrm{d}Q_{\rm dif}(y) = 2\pi y(s/4\pi r^2)(r/L+1)\exp(-r/L)(z/r)\,\mathrm{d}y. \quad (4)$$

The signal profile $q_{\rm dif}(y)$ from the field-free substrate to a unit area along the y direction is written using the total amount of the diffusing minority carriers $Q_{\rm dif}(y)$ as

$$\begin{aligned} 2\pi y\,\mathrm{d}y\,q_{\rm dif}(y) &= Q_{\rm dif}(y) \\ &= \frac{y\mathrm{d}y}{2} I_0 \frac{E}{\varepsilon}\mu\rho \int_{z=0}^{d_{\rm sub}} \exp(-\mu\rho z)\frac{1}{r^2}\left(\frac{r}{L}+1\right) \\ &\quad \times \exp(-r/L)(z/r)\,\mathrm{d}z \\ &= \frac{y\mathrm{d}y}{2} I_0 \frac{E}{\varepsilon}\mu\rho \int_{r=y}^{(y^2+d_{\rm sub}^2)^{1/2}} \exp\left[-\frac{r}{L}-\mu\rho(r^2-y^2)^{1/2}\right] \\ &\quad \times (1/r^2)(r/L+1)\,\mathrm{d}r. \end{aligned} \quad (5)$$

Configurations of the multichannel detector for X-ray tomography diagnostics correspond to the condition of $x_{\rm det} >> L$. The integration over x from $x_{\rm det}/2$ to $-x_{\rm det}/2$ is carried out to take account of the diffusing-charge distribution in the x direction; here, $x_{\rm det}$ is the total width of the detector. Consequently, for the configuration of Fig. 1(a), an output-signal profile from the multichannel detector for unit-intensity X-rays is written as

$$\begin{aligned} J_{\rm SX}(y) = &\int_{x=-x_{\rm det}/2}^{x_{\rm det}/2} (I_0/4\pi)(E/\varepsilon)\mu\rho \\ &\times \int_{r=(y^2+x^2)^{1/2}}^{(y^2+x^2+d_{\rm sub}^2)^{1/2}} (1/r^2)(r/L+1) \\ &\times \exp\left\{-r/L-\mu\rho[r^2-(y^2+x^2)]^{1/2}\right\}\mathrm{d}r\,\mathrm{d}x. \end{aligned} \quad (6)$$

The curves in Fig. 1(b) represent the diffusion signals $J_{\rm sx}(y)$ using our three-dimensional diffusion theory [equation (6)] for a unit-intensity X-ray at 5 keV.

3. Verification of the new diffusion theory and diffusion-length measurements using synchrotron radiation

3.1. *Experimental setup*

The energy of synchrotron radiation at the Photon Factory is changed using a double-crystal [Si(111)] monochromator with a resolution of a few eV (Kohagura *et al.*, 1995). X-rays ranging from 5 to 20 keV are monitored with ionization chambers using nitrogen or argon gas (beamline BL-15C).

For the experiments, we utilize two types of silicon semiconductor detectors. (i) One is a microstrip semiconductor detector having 520 channels fabricated on a 5.2 mm × 5.2 mm × 300 µm-thick silicon wafer (*i.e.* 10 µm width per channel) (Fig. 2a). (ii) Another is an n-type 19-channel detector with a 150 µm wafer thickness. Each channel has an active area of 4.00 mm × 0.90 mm, and is fabricated on one silicon wafer (Snider, 1990). These detectors are characterized by the conditions of (i) $y_{\rm det} << L$, and (ii) $y_{\rm det} >> L$. Here, L is of the order of 100 µm.

A computer-controlled position scanner for the detectors is prepared for precise setting. Reproducible position control in the x, y and θ directions on the detector surface (see Fig. 1a) within the accuracy of 0.5 µm, 0.5 µm and 0.005°, respectively, is achieved along with a goniometric control within 0.002°.

3.2. *Microstrip semiconductor detector*

A rectangularly collimated X-ray beam (240 µm × 3.5 mm) at 9.5 keV is incident onto the microstrip detector. In Fig. 2(b), the data shown by the open and the filled circles are obtained in a fully and a partially depleted operation, respectively.

The summation of the diffusing-signal profile (§2) over the finite beam width (y direction) produces the total diffusion signals $F_d(y)$ for each detector channel at the location of y,

$$\begin{aligned} F_d(y) = &\int_{y_{\rm sou}=|y_{\rm sou1}|}^{|y_{\rm sou2}|} \int_{x=-x_{\rm det}/2}^{x_{\rm det}/2} (I_0/4\pi)(E/\varepsilon)\mu\rho \\ &\times \int_{r=[(y+|y_{\rm sou}|)^2+x^2]^{1/2}}^{[(y+|y_{\rm sou}|)^2+x^2+d_{\rm sub}^2]^{1/2}} (1/r^2)(r/L+1) \\ &\times \exp\left(-r/L-\mu\rho\left\{r^2-[(y+|y_{\rm sou}|)^2+x^2]\right\}^{1/2}\right) \\ &\times \mathrm{d}r\,\mathrm{d}x\,\mathrm{d}y_{\rm sou}. \end{aligned} \quad (7)$$

Here, the width of the incident X-ray beam, $y_{\rm sou}$, is written as $y_{\rm sou} = y_{\rm sou1} - y_{\rm sou2}$; $y_{\rm sou1}$ and $y_{\rm sou2}$ are the locations of both edges of the rectangular X-ray beam.

The curves in Fig. 2(b) represent the diffusion signals $F_d(y)$ for detector channels aligned in the y direction calculated using (7) as a function of L. The anticipated diffusion signal is clearly observed only when the applied bias is reduced and the field-free substrate region is formed. The charges created by X-rays diffuse three-dimensionally in the field-free substrate, while the charges produced in the depletion layer drift along the electric field only

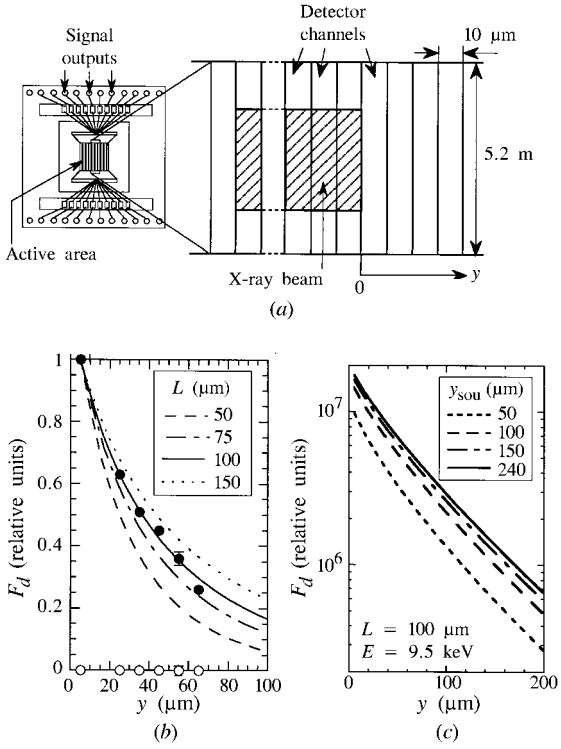

Figure 2
(a) Schematic view of the microstrip detector. The origin of the y coordinates is defined at the position of the edge of the incident X-ray beam. (b) The data shown by the open and filled circles are obtained in a fully depleted and a partially depleted operation, respectively, while, the curves represent the diffusion signals calculated using equation (7) as a function of L. (c) The curves calculated using equation (7) represent the dependence of the diffusion signals on the finite width of an incident X-ray beam $y_{\rm sou}$.

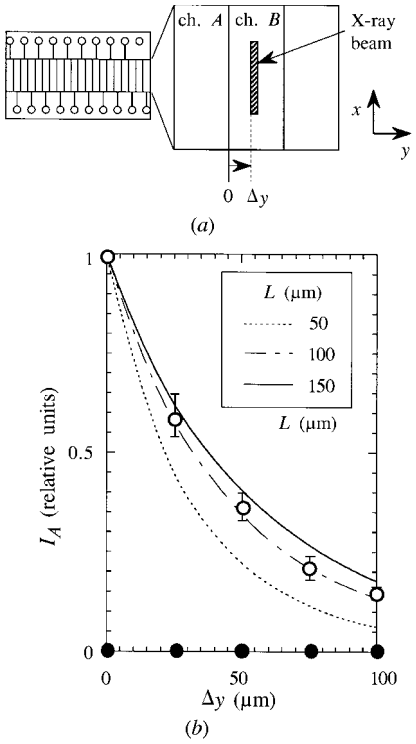

Figure 3
(*a*) Schematic view of the multichannel detector along with the incident X-ray location. (*b*) The output currents from ch. *A* are plotted by the filled and open circles in fully depleted (40 V) and partially depleted (2 V) operations, respectively, while $F_d(y)$ [see equation (7)] is integrated over the total area of ch. *A* for the estimation of the detector signal from ch. *A*. The curves represent calculated signals as a function of *L*.

one-dimensionally without the penetration into the adjoining channels. The curves in Fig. 2(*c*) represent the dependence of the diffusion signals on the incident beam width, y_{sou}. The saturation tendency of the diffusion signals with $y_{sou} > L$ shows no critical contribution of the beam shape or width to utilize the relative slope analyses of F_d, when a beam with $y_{sou} > L$ is employed.

The experimental verification of our novel theory on the semiconductor response will also provide a new method for obtaining the value of *L*, which is one of the most important parameters for semiconductor devices, particularly for industrial requirements. In fact, *L* is an important design factor for the switching time of semiconductor devices. The value of *L* is also cross-checked by the X-ray energy response data using the same method as Cho *et al.* (1992). The response data are fitted using our theoretical formula for the X-ray response; that is, the substitution of only two free parameters in the formula, namely (i) the experimentally obtained value of *L* (see above), and (ii) d_{dep} independently observed from the capacitance–voltage characteristics, results in the theoretical fitting curve. The data are then found to be well fitted by the theoretical curves.

The above results indicate the reliability of our new theory on semiconductor X-ray detector responses; namely, the existence of the physics process of the three-dimensional charge diffusion effect.

3.3. *Multichannel semiconductor detector*

Fig. 3(*a*) shows schematic drawings of the relation between the X-ray beam position and the multichannel-detector location. Incident 10 keV X-rays are collimated in the square shape of 200 μm × 3.5 mm.

X-rays are injected onto channel *B* (ch. *B*) near the boundary between the channels *A* (ch. *A*) and *B* (see Fig. 3*a*). The detector in a fully depleted operation is scanned in the *y* direction, and then positioned using the precise scanner (see §3.2).

After the positioning, we reduce the detector bias to 2 V. This leads to the formation of a 120 μm-thick field-free substrate region. The output signal from ch. *A*, in fact, appears when the bias is reduced.

To obtain the dependence of the signals from ch. *A* on the distance Δy from the channel boundary, we scan the detector in the *y* direction. The data plotted by the open and filled circles in Fig. 3(*b*) show the output signals in the cases of partially depleted (2 V) and fully depleted (40 V) operations, respectively.

On the other hand, this dependence is predicted using our theory. For the estimation of the detector signal from ch. *A* (I_A), $F_d(y)$ [see equation (7)] is integrated over the total area of ch. *A* because of the precise inclusion of the charge profile in ch. *A*. In Fig. 3(*b*), the solid, dot-dashed and dotted curves are calculated using L = 150, 100 and 50 μm, respectively. The open-circle data are fitted by the curve with L = 100 μm. It is noted that this value is consistent with the estimated value using the X-ray energy response of the detector (Cho *et al.*, 1995).

Consequently, our predicted effect of the three-dimensional charge diffusion in multichannel semiconductor detectors is experimentally verified. Here, it is noted that this experimental method is also available to the diffusion-length measurements even for detectors with $y_{det} >> L$.

References

Cho, T. *et al.* (1992). *Phys. Rev. A*, **46**, 3024–3027.
Cho, T. *et al.* (1995). *Rev. Sci. Instrum.* **66**, 540–542.
Hopkinson, G. R. (1983). *Nucl. Instrum. Methods*, A**216**, 423–429.
Kohagura, J. *et al.* (1995). *Rev. Sci. Instrum.* **66**, 2317–2319.
Price, W. J. (1964). *Nuclear Radiation Detection.* New York: McGraw-Hill.
Snider, R. T. (1990). *Nucl. Fusion*, **30**, 2400–2405.
Wenzel, K. W. & Petrasso, R. D. (1988). *Rev. Sci. Instrum.* **59**, 1380–1387.